Contribution from the Department of Chemistry, Northwestern University, Evanston, Illinois 60201,
and Fujian Institute of Research on the Structure of Matter,
Chinese Academy of Sciences, Fuzhou, Fujian, People's Republic of China

New Layered Ternary Chalcogenides: Ta_2PdS_6, Ta_2PdSe_6, Nb_2PdS_6, Nb_2PdSe_6

DOUGLAS A. KESZLER,† PHILIP J. SQUATTRITO,† NATHANIEL E. BRESE,† JAMES A. IBERS,*†
SHANG MAOYU,‡ and LU JIAXI‡

Received September 12, 1984

The new ternary transition-metal chalcogenides Ta_2PdS_6, Ta_2PdSe_6, Nb_2PdS_6, and Nb_2PdSe_6 have been prepared. The phases are isostructural. The structures of the phases Ta_2PdS_6 and Ta_2PdSe_6 have been established by single-crystal X-ray measurements. Ta_2PdS_6: C_{2h}^3-$I2/m$, $Z = 2$, $a = 9.960$ (13) Å, $b = 3.271$ (5) Å, $c = 11.696$ (16) Å, $\beta = 114.51$ (4)°, $V = 346.7$ Å^3, $R(F^2) = 0.070$ for 1202 observations, 30 variables, $R(F) = 0.034$ for 1138 $F_o^2 > 3\sigma(F_o^2)$. Ta_2PdSe_6: C_{2h}^3-$I2/m$, $Z = 2$, $a = 10.423$ (6) Å, $b = 3.375$ (2) Å, $c = 12.196$ (6) Å, $\beta = 113.68$ (2)°, $V = 392.9$ Å^3, $R(F^2) = 0.135$ for 1201 observations, 30 variables, $R(F) = 0.056$ for 696 $F_o^2 > 3\sigma(F_o^2)$. The unit cell parameters of the phases Nb_2PdSe_6 and Nb_2PdS_6 have been determined from single-crystal and powder X-ray measurements, respectively. Nb_2PdSe_6 crystallizes in an I-centered cell of dimensions $a = 10.368$ (1) Å, $b = 3.362$ (1) Å, $c = 12.132$ (2) Å, $\beta = 113.42$ (2)°, $V = 388.0$ Å^3, and $Z = 2$. The compound Nb_2PdS_6 crystallizes in a cell of dimensions $a = 9.99$ (1) Å, $b = 3.30$ (1) Å, $c = 11.69$ (1) Å, $\beta = 114.7$ (1)°, and $V = 350$ Å^3. The phases form in a new laminar structural type. Each layer consists of collocated units $^1_\infty[M_2PdQ_6]$ (M = Ta or Nb; Q = S or Se) that are composed of MQ_3 face-sharing trigonal-prismatic chains bridged by Pd atoms in a square-planar environment of Q atoms. Metrical details and results of electrical conductivity measurements on Ta_2PdQ_6 indicate the simple valence description Ta^V, Pd^{II}, Q^{-II}.

Introduction

The binary transition-metal chalcogenides MQ_3 (M = Ta, Nb; Q = S, Se) are layered materials formed from collocated chains of MQ_3 (Figure 1). The interesting structural[1] and unusual electrical[2] characteristics of these materials have occasioned various experiments in chemical modification. Insertion of Li atoms between the layers has been reported for the phases NbS_3, $NbSe_3$, and $TaSe_3$.[3] As a consequence of the reversibility of Li atom incorporation and high electrical conductivity, the phase $NbSe_3$ has been of considerable interest as a cathode in lithium batteries.[4] In addition to insertion of atoms between the layers of the compound $NbSe_3$, inclusion of the transition metals V, Cr, and Fe occurs within the layers with retention of the $NbSe_3$ chains albeit in the distinct structural type Nb_3FeSe_{10}.[5]

Prompted by these results and our interest in the development of the solid-state chemistry of the Pt-group chalcogenides,[6] we have discovered the new family of compounds Ta_2PdS_6, Ta_2PdSe_6, Nb_2PdS_6, and Nb_2PdSe_6. In this report we describe the synthesis and characterization of this class of materials that crystallize in a new laminar structural type containing simple MQ_3 chains bridged by the ternary atom Pd.

Experimental Section

Ta_2PdSe_6 and Ta_2PdS_6. Single crystals of the materials Ta_2PdSe_6 and Ta_2PdS_6 used in the X-ray investigations (vide infra) were isolated from reactions of high-purity (>99.9%) elements. The combinations of the elements were heated in sealed, evacuated silica tubes at 1050 K for 10 days.

A single-phase homogeneous powder of the material Ta_2PdSe_6 has been prepared. The synthesis of this compound was initiated with reduction of the metals under a flow of H_2 at 600 K for 3 h. The stoichiometric ratio of the elements was loaded into a silica tube that was then evacuated to $\sim 10^{-6}$ torr. The tube was sealed and placed in a tube furnace that was heated from 300 to 825 K at 20 K/h. After radiative cooling, the tube was removed from the furnace and the contents were thoroughly ground under an N_2 atmosphere. The contents were passed through a 270-mesh screen and loaded into a fresh silica tube. After being sealed, the tube was heated at 1000 K for 48 h. This procedure of grinding, sieving, and heating (1000 K) was repeated four times. X-ray powder diffraction data for this sample were obtained with Ni-filtered Cu Kα radiation on a Rigaku Geigerflex powder diffractometer. The experimental trace was in satisfactory agreement with that generated from the known structure (vide infra) by a local version of the computer program LAZY-PULVERIX.[7] The position of each reflection was determined from digitized data obtained by step scanning [100 s/0.01° (2θ)] each reflection. National Bureau of Standards Si Powder Standard Reference Material 640a served as the internal standard.[8] Unit cell parameters were determined from weighted least-squares analysis of 12 reflections in the range $35° < 2\theta < 70°$. The parameters so derived, given in Table I, are in excellent agreement with those derived from a single crystal (vide infra).

The compound Ta_2PdS_6 has also been prepared in powder form. The synthesis was accomplished by reacting stoichiometric amounts of Pd metal and TaS_3, which had been prepared by direct combination of Ta and S heated 24 h at 775 K and 46 h at 925 K. The TaS_3 and Pd powders were loaded into a silica tube that was heated for a total of 60 days at 1000 K with five intermittent grindings. X-ray powder diffraction data for this sample were obtained with Cu Kα radiation on an Enraf-Nonius model FR522 Guinier camera with the use of NBS Si powder (640a) as the standard.[8] Unit cell parameters derived from weighted least-squares analysis of 28 reflections in the range $30° < 2\theta < 70°$, given in Table I, are in satisfactory agreement with those derived from a single crystal (vide infra). Weak lines attributable to TaS_3 were present in the powder pattern, indicating that a small amount of the starting material remained as an impurity.

Nb_2PdSe_6 and Nb_2PdS_6. Single crystals of Nb_2PdSe_6 were isolated from a reaction of the elements heated for 3 weeks at 1075 K in a sealed, evacuated silica tube. Analysis of five crystals with the microprobe of an EDAX-equipped Cambridge S-4 scanning electron microscope affords the composition $Nb_{2.02(3)}Pd_{0.97(3)}Se_{6.01(2)}$. Unit cell parameters were derived from least-squares analysis of 25 reflections automatically centered on an Enraf-Nonius CAD4 X-ray diffractometer. The I-centered cell of dimensions $a = 10.368$ (1) Å, $b = 3.362$ (1) Å, $c = 12.132$ (2) Å, and $\beta = 113.42$ (2)° with a volume of 388.0 Å^3 is consistent with two formula units per cell.

The compound Nb_2PdSe_6 has also been prepared in powder form. A stoichiometric ratio of the elements was heated in a sealed evacuated silica tube for a total of 60 days at 1000 K with four intermittent grindings. During the first grinding, performed after heating for 7 days,

---

† Northwestern University.

‡ Chinese Academy of Sciences.

[1] (a) Rijnsdorp, J.; Jellinek, F. *J. Solid State Chem.* **1978**, *25*, 325–328. (b) Hodeau, J. L.; Marezio, M.; Roucau, C.; Ayroles, R.; Meerschaut, A.; Rouxel, J.; Monceau, P. *J. Phys. C* **1978**, *11*, 4117–4134. (c) Meerschaut, A.; Guemas, L.; Rouxel, J. *J. Solid State Chem.* **1981**, *36*, 118–123. (d) Bjerkelund, E.; Fermor, J. H.; Kjekshus, A. *Acta Chem. Scand.* **1966**, *20*, 1836–1842.

[2] See, for example: Wilson, J. A. *Phys. Rev. B: Condens. Matter* **1979**, *19*, 6456–6468 and references cited therein.

[3] (a) Chianelli, R. R.; Dines, M. B. *Inorg. Chem.* **1975**, *14*, 2417–2421. (b) Murphy, D. W.; Trumbore, F. A. *J. Electrochem. Soc.* **1976**, *123*, 960–964. (c) Broadhead, J.; Trumbore, F. A. *Power Sources* **1974**, *5*, 661–682.

[4] (a) Murphy, D. W.; Trumbore, F. A. *J. Cryst. Growth* **1977**, *39*, 185–199. (b) Trumbore, F. A. *Pure Appl. Chem.* **1980**, *52*, 119–134. (c) Broadhead, J.; Trumbore, F. A.; Basu, S. *J. Electroanal. Chem. Interfacial Electrochem.* **1981**, *118*, 241–250.

[5] (a) Cava, R. J.; Himes, V. L.; Mighell, A. D.; Roth, R. S. *Phys. Rev. B: Condens. Matter* **1981**, *24*, 3634–3637. (b) Meerschaut, A.; Gressier, P.; Guemas, L.; Rouxel, J. *Mater. Res. Bull.* **1981**, *16*, 1035–1040.

[6] (a) Keszler, D. A.; Ibers, J. A. *Inorg. Chem.* **1983**, *22*, 3366–3367. (b) Keszler, D. A.; Ibers, J. A. *J. Solid State Chem.* **1984**, *52*, 73–79. (c) Keszler, D. A.; Ibers, J. A.; Shang, M.; Lu, J. *J. Solid State Chem.* **1985**, *57*, 68–81.

[7] Yvon, K.; Jeitschko, W.; Parthe, E. *J. Appl. Crystallogr.* **1977**, *10*, 73–74.

[8] Hubbard, C. R. *J. Appl. Crystallogr.* **1983**, *16*, 285–288.

0020-1669/85/1324-3063$01.50/0 © 1985 American Chemical Society

Table I. Unit Cell Parameters for Ta_2PdS_6, Ta_2PdSe_6, Nb_2PdS_6, and Nb_2PdSe_6[a]

compd	sample	a, Å	b, Å	c, Å	β, deg	V, Å^3
Ta_2PdS_6	single cryst	9.960 (13)	3.271 (5)	11.696 (16)	114.51 (4)	346.7
Ta_2PdS_6	powder	9.971 (8)	3.272 (3)	11.683 (11)	114.60 (6)	346.6
Ta_2PdSe_6	single cryst	10.423 (6)	3.375 (2)	12.196 (6)	113.68 (2)	392.9
Ta_2PdSe_6	powder	10.420 (2)	3.3761 (5)	12.205 (3)	113.68 (1)	393.2
Nb_2PdS_6	powder	9.99 (1)	3.30 (1)	11.69 (1)	114.7 (1)	350
Nb_2PdSe_6	single cryst	10.368 (1)	3.362 (1)	12.132 (2)	113.42 (2)	388.0
Nb_2PdSe_6	powder	10.357 (5)	3.362 (2)	12.141 (6)	113.48 (5)	387.7

[a] The angles α and γ were constrained to be zero in refinements of the cells.

Table II. Summary of Crystal Data and Intensity Collection

	Ta_2PdS_6	Ta_2PdSe_6
mol wt	660.68	942.06
space group	C_{2h}^3-$I2/m$	C_{2h}^3-$I2/m$
Z	2	2
T of data collcn, K	298	298
radiation[c]	Mo Kα	Mo Kα
cryst shape	flattened rod, bound by $\{101\}$, $\{10\bar{1}\}$, $\{010\}$, $\{10\bar{3}\}$, $\{100\}$, (102), and (104)	flattened rod, bound by $\{101\}$, $\{10\bar{1}\}$, $\{010\}$, $\{10\bar{3}\}$, (100), $(30\bar{1})$, $(\bar{1}02)$, and (001)
cryst vol, mm^3	0.000 68	0.000 26
linear abs coeff, cm^{-1}	352	571
transmission factors[a]	0.216–0.423	0.094–0.396
detector aperture, mm	horiz slit 3; vert slit 3.5 + 1.50 tan θ, 17.3 cm from cryst	horiz slit 3; vert slit 1.5 + 1.05 tan θ, 17.3 cm from cryst
takeoff angle, deg	4.0	3.0
scan speed,[b] deg min^{-1}	1.33 in ω ($0° \leqslant 2\theta \leqslant 80°$)	2.0 in ω ($2° \leqslant 2\theta \leqslant 60°$) 1.33 in ω ($60° < 2\theta < 76°$)
scan range, deg	1.0 below Kα_1 to 1.0 above Kα_2	1.0 below Kα_1 to 1.0 above Kα_2
bkgd counts	$^1/_4$ of scan range on each side of reflcn	$^1/_4$ of scan range on each side of reflcn
λ^{-1} sin θ, Å^{-1}	0.0246–0.9062	0.0246–0.8680
limits	$2.0° \leq 2\theta$(Mo Kα_1) $\leq 80°$	$2.0° \leq 2\theta$(Mo Kα_1) $\leq 76°$
data collcd	$\pm h,\pm k,\pm l$ ($0° \leqslant 2\theta \leqslant 40°$) $\pm h,+k,+l$ ($40° \leqslant 2\theta \leqslant 80°$)	$\pm h,\pm k,\pm l$ ($2° \leqslant 2\theta \leqslant 40°$) $+h,+k,\pm l$ ($40° < 2\theta \leqslant 76°$)
p factor	0.04	0.04
no. of unique data (including $F_o^2 < 0$)	1202	1201
no. of unique data with $F_o^2 \geq 3\sigma(F_o^2)$	1138	696
$R(F^2)$	0.070	0.135
$R_w(F^2)$	0.085	0.156
R (on F for $F_o^2 > 3\sigma(F_o^2)$)	0.034	0.056
error in observn of unit wt, e^2	1.67	1.35

[a] The analytical method, as employed in the Northwestern absorption program AGNOST, was used for the absorption correction (de Meulenaer, J.; Tompa, H. *Acta Crystallogr.* **1965**, *19*, 1014–1018). [b] Reflections for which $\sigma(I)/I > 0.3$ were rescanned to a maximum time of scan of 180 s. [c] Graphite monochromatized.

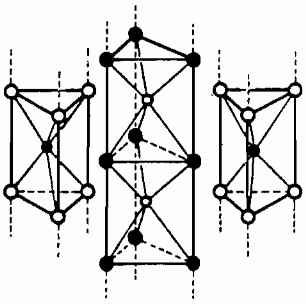

Figure 1. Collocated chains in MQ_3 (M = Nb, Ta; Q = S, Se).

a small excess of Se (~3 wt %) was added to the sample, which was then reloaded into a fresh silica tube and heated for 19 days at 1000 K. After this second heating, the excess Se was sublimed off to the transport end of the tube across a 775–298 K temperature gradient over 6 min. No additional Se was added to the sample during subsequent grindings. X-ray powder diffraction data for this sample were obtained as described above for Ta_2PdS_6. Weighted least-squares analysis of 24 reflections in the range $30° < 2\theta < 70°$ yielded unit cell parameters, given in Table I, that are in excellent agreement with those derived from a single crystal. The powder pattern also contained lines attributable to the structural type $Nb_2Pd_{0.71}Se_5$,[6c] indicating that the sample was inhomogeneous.

Direct combination of a stoichiometric ratio of Nb, Pd, and S, heated in a sealed, evacuated silica tube at 1000 K for a total of 60 days with five intermittent grindings, yielded a powder sample whose X-ray powder diffraction pattern was obtained as for Ta_2PdS_6 and Nb_2PdSe_6. The unit cell parameters derived from weighted least-squares analysis of 10 reflections in the range $30° < 2\theta < 70°$ are a = 9.99 (1) Å, b = 3.30 (1) Å, c = 11.69 (1) Å, β = 114.7 (1)°, and V = 350 Å^3. The powder pattern, whose quality was inferior to the others discussed here, contained several weak, unidentified lines, indicating that the sample was not completely homogeneous.

Crystallographic Studies. The phase Ta_2PdSe_6 was assigned to Laue group $2/m$ from examination of Weissenberg X-ray photographs. The systematic absence (hkl, $h + k + l = 2n + 1$) is consistent with the space groups C_{2h}^3-$I2/m$, C_s^3-Im, and C_2^3-$I2$. As a satisfactory residual of 0.035 results from averaging of the hkl, $\bar{h}\bar{k}\bar{l}$ pairs for the inner sphere of absorption-corrected data, the group $I2/m$ is favored. A less satisfactory residual of 0.063 obtains upon inclusion of the absorption-corrected equivalent reflections $\bar{h}k\bar{l}$ and $h\bar{k}l$ in the averaging procedure. Since the crystal used for collection of the X-ray data possessed an approximate morphological center of symmetry, agreement between the hkl and $\bar{h}\bar{k}\bar{l}$ pairs is less dependent on absorption corrections. The poorer agreement between hkl and $h\bar{k}l$ pairs is probably a result of the high absorption of the material (μ = 571 cm^{-1}) and possible imperfections on the surface of the crystal. The cell parameters were determined from least-squares analysis of 25 reflections in the range $26° \leq 2\theta$ (Mo Kα_1) $\leq 45°$ that had been automatically centered on an Enraf-Nonius CAD4 X-ray diffractometer. The refined cell constants are given in Table I, and additional relevant crystal data are given in Table II.

Intensity data were collected at room temperature with the ω–2θ scan technique. The intensities of six standard reflections, measured every 2 h throughout data collection, were stable. Initial calculations were performed on a VAX 11/730 computer with the use of the Enraf-Nonius CAD4-SDP programs.[9] The atoms Pd, Ta, and Se(1) were located from

---

[9] The crystallographic computing package is described in: Frenz, B. A. "Computing in Crystallography"; van Konigsveld, H., Bassi, G. C., Eds.; Delft University Press: Delft, Holland, 1983; p 64.

Table III. Positional Parameters and Equivalent Isotropic Thermal Parameters for Ta_2PdS_6 and Ta_2PdSe_6

atom	*x*	*y*	*z*	B_{eq}, Å^2
		Ta_2PdS_6		
Ta	0.391 187 (25)	0	0.684 861 (21)	0.5
Pd	0	0	0	0.8
S(1)	0.729 75 (18)	$^1/_2$	0.488 71 (14)	0.7
S(2)	0.118 82 (17)	0	0.658 73 (14)	0.7
S(3)	0.591 82 (17)	$^1/_2$	0.719 04 (15)	0.7
		Ta_2PdSe_6		
Ta	0.390 235 (96)	0	0.679 992 (84)	0.6
Pd	0	0	0	1.0
Se(1)	0.732 80 (23)	$^1/_2$	0.494 11 (20)	0.9
Se(2)	0.118 94 (23)	0	0.658 48 (20)	0.8
Se(3)	0.593 30 (24)	$^1/_2$	0.718 51 (20)	0.9

a Patterson synthesis. The remaining Se atoms were located from an ensuing electron density synthesis. All further calculations were performed on a Harris 800 computer with methods standard for this laboratory.[10] Scattering factors and anomalous dispersion terms were taken from the usual sources.[11] The final cycle of refinement was performed on F_o^2 and included all 1201 reflections. The final residuals R and R_w on F_o^2 are 0.135 and 0.156, respectively. Other residuals are given in Table II. A final difference electron density map reveals no features greater than 0.7% of a Ta atom. An analysis of F_o^2 vs. F_c^2 as a function of $\lambda^{-1} \sin \theta$, F_o^2, and Miller indices reveals no unusual trends. Final positional parameters are provided in Table III. Final anisotropic thermal parameters and structure amplitudes are given in Tables IV[12] and V,[12] respectively.

Analysis of Weissenberg photographs reveals that crystals of Ta_2PdS_6 also belong to the monoclinic system. The systematic absence (hkl, $h + k + l = 2n + 1$) is indicative of the space groups C_{2h}^3-$I2/m$, C_s^3-Im, and C_2^3-$I2$. As a satisfactory agreement index of 0.023 results from averaging the inner sphere of absorption-corrected data in space group $I2/m$, this group is favored. The lattice parameters were determined from least-squares analysis of the setting angles of 25 reflections in the range 12° $< 2\theta$ (Mo Kα_1) $<$ 25° automatically centered on an Enraf-Nonius CAD4 diffractometer. Six standard reflections monitored every 4 h exhibited no significant changes during the course of data collection. Refined unit cell parameters are given in Table I, and crystallographic details are summarized in Table II.

From the cell parameters and probable space group, we assumed this phase to be isostructural with the compound Ta_2PdSe_6. The initial atomic parameters for refinement were therefore taken from the selenide. The final cycle of refinement performed on F_o^2 with all 1202 unique reflections afforded residuals $R = 0.070$ and $R_w = 0.085$. Other residuals may be found in Table II. No unusual trends are observed from an analysis of F_o^2 vs. F_c^2 as a function of F_o^2, $\lambda^{-1} \sin \theta$, and Miller indices. The final difference electron density map exhibits no features with height greater than 1.7% of a Ta atom.

Final atomic parameters are provided in Table III. Anisotropic thermal parameters and structure amplitudes are given in Tables VI[12] and VII,[12] respectively. The anisotropic thermal parameters for Ta_2PdS_6 and Ta_2PdSe_6 are unexceptional and thus provide strong support for the ordered nature of these structures.

Conductivity Measurements. Four-probe single-crystal conductivity measurements were made along *b*, the needle axis, with procedures described previously.[13]

Results

The results of the single-crystal studies indicate that the compounds Ta_2PdS_6 and Ta_2PdSe_6 are two members of an isomorphous series of new materials. The unit cell parameters and Bravais lattice type derived from a single crystal of Nb_2PdSe_6 suggest that it is isostructural with the Ta analogues. In addition, the X-ray diffraction pattern of the Nb_2PdS_6 powder sample is in satisfactory agreement with that generated from the positional parameters of Ta_2PdS_6. Hence, this compound is also part of this isomorphous series.

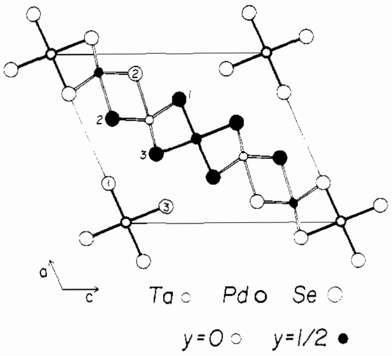

Figure 2. Projection of the structure of Ta_2PdSe_6 onto the *a*–*c* plane showing the labeling scheme.

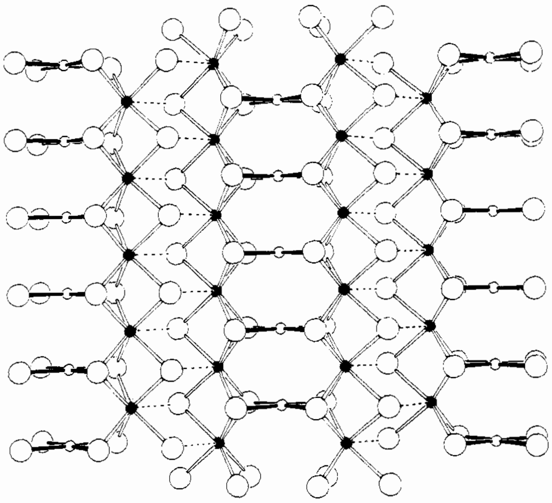

Figure 3. Drawing of an individual layer $^2_\infty[Ta_2PdSe_6]$ as viewed orthogonal to (101). Ta atoms are small filled circles, Pd atoms are small open circles, and Se atoms are large open circles.

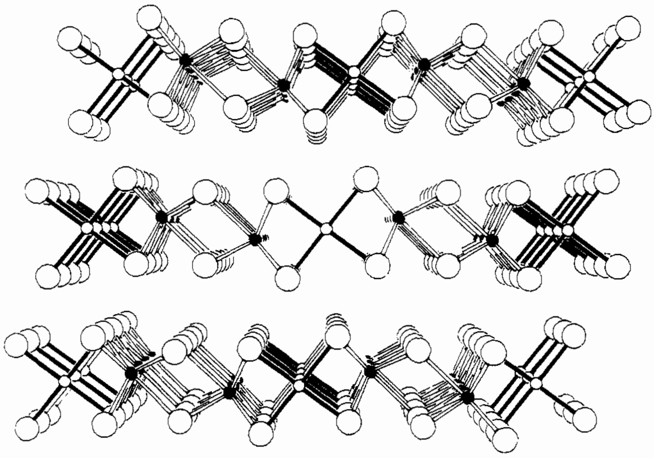

Figure 4. Perspective view of Ta_2PdSe_6 along [010]. Ta atoms are small filled circles, Pd atoms are small open circles, and Se atoms are large open circles.

The materials form with a new layered-type structure with the layers paralleling the plane (101). A projection of this structural type, Ta_2PdSe_6, onto the *a*–*c* plane is given in Figure 2. A drawing of an individual layer as viewed orthogonal to (*101*) appears in Figure 3. The layer may be viewed as consisting of individual units of composition $^1_\infty[M_2PdQ_6]$. Each unit consists of two columns of M-centered face-sharing Q trigonal prisms bridged by the Pd atoms. Each layer is then realized by juxtaposition of these units through the relative displacement *b*/2, as emphasized by the dashed lines of Figure 3. This disposition of the units results

---

(10) For example: Waters, J. M.; Ibers, J. A. *Inorg. Chem.* **1977**, *16*, 3273–3277.

(11) Cromer, D. T.; Waber, J. T. "International Tables for X-ray Crystallography"; Kynoch Press: Birmingham, England 1974; Vol. IV, Table 2.2A. Cromer, D. T. *Ibid.* Table 2.3.1.

(12) Supplementary material.

(13) Phillips, T. E.; Scaringe, R. P.; Hoffman, B. M.; Ibers, J. A. *J. Am. Chem. Soc.* **1980**, *102*, 3435–3444.

Table VIII. Selected Bond Distances (Å) and Angles (deg) for Ta_2PdS_6 and Ta_2PdSe_6[a]

	Q = S	Q = Se		Q = S	Q = Se
Pd–2Q(3)	2.336 (4)	2.442 (3)	Q(3)–2Q(3)	3.352 (5)	3.477 (5)
Pd–2Q(1)	2.346 (4)	2.456 (3)	Q(2)–2Q(2)	3.071 (4)	3.224 (3)
Pd–2Pd	3.271 (5)	3.375 (2)	Q(2)–Q(3)	2.989 (4)	3.132 (4)
Pd–4Ta	3.236 (2)	3.316 (1)	Q(1)–Pd–Q(3)	83.43 (8)	86.15 (8)
Ta–2Q(1)	2.494 (2)	2.610 (2)	Q(1)–Ta–Q(3)	77.51 (9)	79.93 (6)
Ta–2Q(2)	2.487 (3)	2.625 (2)	Q(2)–Ta–Q(2)	74.24 (5)	73.96 (6)
Ta–2Q(3)	2.483 (3)	2.598 (2)	Q(1)–Ta–Q(1)	81.98 (12)	80.59 (7)
Ta–Q(2)	2.601 (4)	2.733 (3)	Q(2)–Ta–Q(3)	73.94 (9)	73.69 (8)
Ta–2Ta	3.271 (5)	3.375 (2)	Q(3)–Ta–Q(3)	82.41 (13)	81.04 (9)
Ta–2Pd	3.236 (2)	3.316 (1)	Q(1)–Ta–Q(2)	77.07 (7)	76.75 (7)
Ta–2Ta	4.057 (4)	4.280 (2)	Q(2)–Ta–Q(2)	82.27 (13)	80.04 (9)

[a] These values were calculated from the unit cell parameters derived from single crystals (Table I).

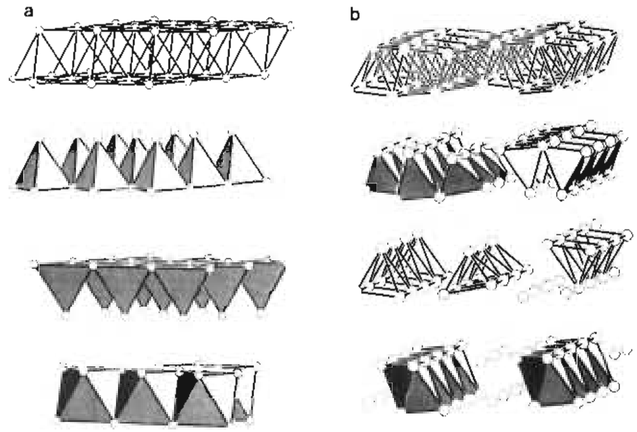

Figure 5. (a) Vacant sites in the van der Waals' gap of TaQ_2. The nature of the gap, tetrahedra pointing "up", tetrahedra pointing "down", and octahedra, respectively, are depicted. (b) Vacant sites in the van der Waals' gap of Ta_2PdQ_6. The nature of the gap and some vacant tetrahedral, square-pyramidal, and octahedral sites, respectively, are depicted.

in a monocapped trigonal-prismatic environment of Q atoms about the M atoms. As shown in Figure 4, the full nature of the structure is realized by stacking the layers along the direction [101] in a pseudo-closest-packed manner. This stacking affords the van der Waals' gap characteristically associated with a laminar structural type.

Metrical details for the phases Ta_2PdS_6 and Ta_2PdSe_6 appear in Table VIII. The Pd–Q and Ta–Q distances are consistent with similar interactions in the materials $PdSe_2$,[14] PdS_2,[14] PdS,[15] $Nb_2Pd_3Se_8$,[6b] $Ta_2Pd_3Se_8$,[6c] TaS_3,[1c] and $TaSe_3$.[1d] The metallic environment of each Pd atom includes two Pd atoms at one unit translation along *b* away and four equidistant Ta atoms (Figure 3). Each Ta atom is adjacent to two Ta atoms at one unit translation along *b*, two nearest-neighbor Pd atoms, and two more distant Ta atoms across the edges formed by the capping Se atoms (Figure 3). Among the metal–metal distances, the Ta–Pd distances are the shortest (Table VIII).

The chalcogen atoms are each bound to three metal atoms. The S–S distances within the layers of Ta_2PdS_6 range from 2.989 (4) to 3.546 (6) Å, and similarly, the intralayer Se–Se distances of Ta_2PdSe_6 range from 3.132 (4) to 3.578 (4) Å. These distances are considerably longer than the S–S distances 2.105 (4) and 2.068 (3) Å observed in the material TaS_3[1c] and the Se–Se distances 2.374 (4) and 2.485 (5) Å observed in the phase $NbSe_3$[1b] that are indicative of Q–Q bonding. Although the S···S distances, 3.352 (5)–3.906 (5) Å, and the Se···Se distances, 3.477 (5)–4.072 (3) Å, across the van der Waals' gap are similar to those observed in the materials TaQ_3, the nature of the gap is very different because of the absence of Q–Q bonding. These S···S and Se···Se distances may also be compared with similar interactions encountered across the van der Waals' gap of the layered dichalcogenides 4H-TaS_2,[16] 3.22 Å, and 4H-$TaSe_2$,[17] 3.45 (3) Å. The longer S···S and Se···Se distances observed in Ta_2PdS_6 and Ta_2PdSe_6 arise in part from the necessarily less regular and less efficient packing of the layers. As shown in Figure 5, the closest packing of atoms, as occurs for the van der Waals' gap of the layered dichalcogenides, affords the characteristic tetrahedral interstices that point "up" or "down" and the two-dimensional edge-sharing array of octahedral sites. For the ternary materials Ta_2PdS_6 and Ta_2PdSe_6, we observe, in addition to distorted tetrahedral sites that point "up" or "down" and edge-sharing octahedral sites, a series of tetrahedral sites formed from two vertices in the "upper" layer and two vertices in the "lower" layer. Moreover, the packing of the layers affords a series of vacant square-pyramidal sites (Figure 5b) that are not observed in the van der Waals' gap of the layered dichalcogenides.

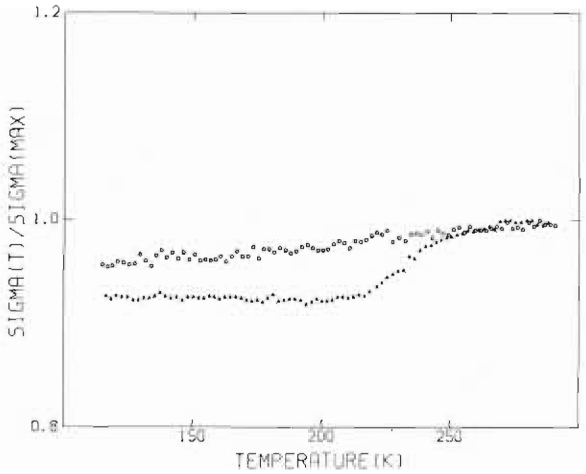

Figure 6. Conductivity behavior vs. temperature (K) for Ta_2PdS_6 (triangles) and Ta_2PdSe_6 (squares). Conductivities have been normalized to the maximum conductivity observed for each crystal. These maxima were 241 Ω^{-1} cm^{-1} at 271 K for Ta_2PdS_6 and 481 Ω^{-1} cm^{-1} at 285 K for Ta_2PdSe_6.

The characteristic structural features of these materials then are the presence of collocated chains of MQ_3 units without Q–Q bonding and the irregular and open van der Waals' gap that results from a deviation in closest packing of the chalcogen atoms. From the simple structural nature of the materials Ta_2PdS_6 and Ta_2PdSe_6 we may formulate an equally simple valence description of Ta^V, Pd^{II}, Q^{-II}. With this formal valence description the electronic levels of the atoms are energetically arranged in the increasing order Q < Pd < Ta. If the metal atoms are considered to be d^8 Pd^{II} and d^0 Ta^V, then at the Fermi level substantial Pd orbital character is anticipated. Of importance above these occupied states would be the empty Ta d levels and an additional Pd d band that results from the orbital directed toward the Se atoms of the square plane. The existence of an energy gap between the occupied Pd levels and the higher empty orbitals would afford a semiconducting behavior for these materials. Such behavior is also expected from the electron count as each phase has an even number of valence electrons.

The results of electrical conductivity measurements for crystals of Ta_2PdS_6 and Ta_2PdSe_6 are given in Figure 6. The magnitude of the conductivity varied among the crystals measured, but typically is 10^2 Ω^{-1} cm^{-1} for both the sulfide and the selenide. The conductivity is independent of temperature in the range measured. Considering the structural results and these limited transport data, we believe that these materials are dengerate semiconductors. The observed behavior probably arises from incorporation of additional atoms between the layers or from the presence of Q defects within the layers. However, we cannot discount the possibility that the minimum of the conduction band falls below the maximum of the

---

(14) Grønvold, F.; Røst, E. *Acta Crystallogr.* **1957**, *10*, 329–331.

(15) (a) Gaskell, T. F. *Z. Kristallogr.* **1937**, *96*, 203–213. (b) Brese, N. E.; Squattrito, P. J.; Ibers, J. A. *Acta Crystallogr.*, in press.

(16) Jellinek, F. *J. Less-Common Met.* **1962**, *4*, 9–15.

(17) Brown, D. E.; Beerntsen, D. J. *Acta Crystallogr.* **1965**, *18*, 31–36.

valence band as would occur for a semimetal.

These new layered chalcogenides have Ta or Nb in a high formal oxidation state; this should afford a set of empty d orbitals capable of accepting electrons. As with other layered transition-metal chalcogenides, insertion of electron donors into the van der Waals' gap may be possible. Moreover the presence of electron-rich Pd atoms within the layers may allow for insertion of electron acceptors under appropriate experimental conditions. To date we have found an extensive chemistry associated with the layers themselves; these results will be summarized in a forthcoming report.[18]

Acknowledgment. This research was supported by the National Science Foundation, Solid State Chemistry, Grant No. DMR83-15554. Some of the powder measurements were made in the X-ray Facility of Northwestern University's Material Research Center, supported in part under the NSF–MRL program (Grant No. DMR82-16972). S.M. thanks Academia Sinica and the U.S.–China program of the National Science Foundation (Grant No. INT81-17267) for support.

Registry No. Ta_2PdS_6, 97314-96-0; Ta_2PdSe_6, 97314-97-1; Nb_2PdS_6, 97314-94-8; Nb_2PdSe_6, 97314-95-9.

Supplementary Material Available: Tables of anisotropic thermal parameters and structure amplitudes (×10) for Ta_2PdSe_6 (Tables IV and V) and Ta_2PdS_6 (Tables VI and VII) (14 pages). Ordering information is given on any current masthead page.

---

(18) Keszler, D. A.; Ibers, J. A. *J. Am. Chem. Soc.*, in press.

Contribution from the Lehrstuhl für Anorganische Chemie I, Ruhr-Universität, D-4630 Bochum, FRG,
and Anorganisch-Chemisches Institut der Universität, D-6900 Heidelberg, FRG

Preparation and Crystal Structure of Bis(1,4,7-trithiacyclononane)iron(II) Bis(hexafluorophosphate) Containing an Octahedral, Low-Spin $Fe^{II}S_6$ Core. Electrochemistry of $[M([9]aneS_3)_2]^{2+}$ Complexes (M = Fe, Co, Ni)

KARL WIEGHARDT,*[†] HEINZ-JOSEF KÜPPERS,[†] and JOHANNES WEISS[‡]

Received December 6, 1984

The preparation of red $[Fe^{II}([9]aneS_3)_2](PF_6)_2$ ($[9]aneS_3$ = 1,4,7-trithiacyclononane, $C_6H_{12}S_3$) containing an octahedral, low-spin $Fe^{II}S_6$ core is reported. The compound crystallizes in the monoclinic space group $P2_1/c$ with $a = 7.636$ (1) Å, $b = 10.314$ (2) Å, $c = 15.445$ (4) Å, $\beta = 92.96$ (2)°, $V = 1215$ (1) Å^3, and $d_{calcd} = 1.931$ g/cm^3 for $Z = 2$ and molecular weight 706.5. Least-squares refinement of the structure based on 2977 observations led to final discrepancy indices of $R = 0.045$ and $R_w = 0.049$. The structure consists of discrete cations $[Fe([9]aneS_3)_2]^{2+}$, with a nearly regular octahedral FeS_6 core, and PF_6^- anions. The electronic solution spectrum is consistent with a d^6 low-spin electronic configuration. The ligand field strength of $[9]aneS_3$ is comparable with that of its nitrogen analogues 1,4,7-triazacyclononane and 2,2′-bipyridine. Cyclic voltammograms of $[Fe([9]aneS_3)_2]^{2+}$ and $[Ni([9]aneS_3)_2]^{2+}$ in acetonitrile exhibit a reversible and a quasi-reversible one-electron-transfer reaction, respectively, at +0.98 and +0.97 V vs. Fc^+/Fc, which is similar to the irreversible oxidation of the uncoordinated ligand (E_{ox} = +0.99 V vs. Fc^+/Fc). Oxidation of a coordinated ligand is suggested rather than oxidation of the metal centers. In contrast, the cyclic voltammogram of $[Co([9]aneS_3)_2]^{2+}$ exhibits two reversible one-electron-transfer processes at formal redox potentials of −0.013 and −0.86 V vs. Fc^+/Fc, which correspond to the couples $[Co([9]aneS_3)_2]^{3+/2+}$ and $[Co([9]aneS_3)_2]^{2+/+}$, respectively. Magnetic susceptibility measurements indicate a low-spin d^7 configuration ($t_{2g}{}^6e_g{}^1$) for $[Co([9]aneS_3)_2]^{2+}$ and a d^6 low-spin arrangement ($t_{2g}{}^6e_g{}^0$) for $[Fe([9]aneS_3)_2]^{2+}$, whereas $[Ni([9]aneS_3)_2]^{2+}$ is paramagnetic with two unpaired electrons per Ni(II).

Introduction

It has been recognized recently that the cyclic triamine 1,4,7-triazacyclononane exerts a surprisingly high ligand field (LF) strength, the origin of which is controversial.[1-3] The preparation and structural characterization of the octahedral low-spin iron(II) and iron(III) bis complexes[4] $[Fe([9]aneN_3)_2]^{2+}$ and $[Fe([9]aneN_3)_2]^{3+}$ have supported the view that this is a real electronic effect.

In contrast, the coordination chemistry of the trithia analogue 1,4,7-trithiacyclononane ($[9]aneS_3$) has been explored to a much lesser degree due to the prohibitively low yields of the original syntheses.[5,6] Sellmann et al. have recently published an elegant template synthesis for this interesting ligand in good yields.[7]

It is of interest to compare the LF strength of this facially coordinating ligand with that of its nitrogen-donor analogue. Simple thioether ligands are usually considered to be weak ligands.[8] We here report the synthesis, electrochemistry, and crystal structure of the low-spin complex $[Fe([9]aneS_3)_2]^{2+}$. In addition, we have further characterized the complexes $[Ni([9]aneS_3)_2]^{2+}$ and $[Co([9]aneS_3)_2]^{2+}$[6] by their electronic spectra and magnetic moment measurements.

Experimental Section

Materials. The ligand 1,4,7-trithiacyclononane was synthesized by Sellmann's method.[7] $[Ni([9]aneS_3)_2](BF_4)_2$ and $[Co([9]aneS_3)_2](BF_4)_2$ were prepared by the literature procedure.[6]

Preparation of $[Fe([9]aneS_3)_2](ClO_4)_2$. (a) To a solution of 1,4,7-trithiacyclononane ($[9]aneS_3$) (0.18 g) in 20 mL of methanol was added with stirring a solution of $Fe(ClO_4)_3 \cdot 6H_2O$ (0.26 g) in 10 mL of methanol. This solution was heated for 4 h to 50 °C, during which time its color changed to purple. Purple crystals precipitated upon cooling to 0 °C, which were filtered off, washed with ethanol and ether, and air-dried. Recrystallization from a minimum amount of water was achieved by addition of $NaClO_4$, and the hexafluorophosphate salt was precipitated by addition of $NaPF_6$.

(b) An identical product was obtained from argon-scrubbed methanolic solutions of $FeCl_2 \cdot 4H_2O$ with the same reaction conditions as described above. Anal. Calcd for $C_{12}H_{24}S_6FeCl_2O_8$: C, 23.13; H, 4.14; S, 30.28; Fe, 9.35. Found: C, 23.3; H, 3.9; S, 30.8; Fe, 9.1. ^1H NMR (60 MHz, Me_2SO-d_6): $\delta(CH_2)$ = 3.01 (s).

[†] Ruhr-Universität.

[‡] Universität Heidelberg.

(1) Yang, R.; Zompa, L. J. *Inorg. Chem.* **1976**, *15*, 1499.

(2) Alper, J. S.; Zompa, L. J. *J. Inorg. Nucl. Chem.* **1980**, *42*, 1693.

(3) Hart, S. M.; Boeyens, J. C. A.; Hancock, R. D. *Inorg. Chem.* **1983**, *22*, 982.

(4) (a) Wieghardt, K.; Schmidt, W.; Herrmann, W.; Küppers, H.-J. *Inorg. Chem.* **1983**, *22*, 2953. (b) Boeyens, J. C. A.; Forbes, A.; Hancock, R. D.; Wieghardt, K. *Inorg. Chem.*, in press.

(5) (a) Gerber, D.; Chongsawangvirod, P.; Leung, A. K.; Ochrymowycz, L. A. *J. Org. Chem.* **1977**, *42*, 2645. (b) Glass, R. S.; Wilson, G. S.; Setzer, W. N. *J. Am. Chem. Soc.* **1980**, *102*, 5068.

(6) Setzer, W. N.; Ogle, C. A.; Wilson, G. S.; Glass, R. S. *Inorg. Chem.* **1983**, *22*, 266.

(7) Sellmann, D.; Zapf, L. *Angew. Chem.* **1984**, *96*, 799. *Angew. Chem., Int. Ed. Engl.* **1984**, *23*, 807.

(8) Murray, S. G.; Hartley, F. R. *Chem. Rev.* **1981**, *81*, 365.

0020-1669/85/1324-3067$01.50/0 © 1985 American Chemical Society